Computer-aided analysis and simulation of complex passive integrated optical circuits of arbitrary rectilinear topology

Gürkan Önal
Ayhan Altintaş, MEMBER SPIE
Haldun M. Ozaktas
Bilkent University
Department of Electrical and Electronics Engineering
06533 Bilkent
Ankara, Turkey
E-mail: haldun@ee.bilkent.edu.tr

Abstract. Optical interconnections can be beneficially employed at the chip-to-chip or backplane level of high-performance computing systems. One method of providing high speed and density interconnections among a large number of integrated circuit chips is with a passive integrated optics circuit. We have developed a method of breaking down arbitrarily complex rectilinear circuits into elementary blocks whose loss and coupling properties are known. Thus, the overall loss and noise for each connection can be calculated. A high-speed algorithm based on this method has been implemented. The high speed of our analysis system makes it suitable for incorporation in an iterative design system, which determines the minimum spacings between the guides and results in acceptable crosstalk and noise levels.

Subject terms: optical interconnects and packaging; integrated optics.

Optical Engineering 33(5), 1596–1603 (May 1994).

1 Introduction

It has been widely argued that the use of optical interconnections may provide several benefits over electrical interconnections in many situations.[1–7] Comparisons of performance characteristics—such as speed, bandwidth, power consumption, and footprint area—of electrical and optical or optoelectronic circuits have been published.[8–12] Some particular examples of practical implementations of optical interconnections are a multifiber bus for module-to-module connections, a mastercard for a backplane, waveguide arrays for multichip modules, and a chip-level clock distribution demonstrator for chip-level optical interconnections.[13]

Single-mode channel waveguides can be made the basis of an integrated optics approach to providing optical interconnections (Ref. 14, p. 59). Materials such as silicon nitride[15] or various polymers[16,17] can be used to realize the passive waveguides. Waveguide interconnects between chips on a multichip module, between individual chips or multichip modules on a printed circuit board, and between boards attached to a backplane have previously been studied.[18] Commercial simulation tools for analyzing channel waveguides have already been developed that are mostly based on the beam propagation method.[19,20]

Despite these and similar efforts, we are not aware of any general approach toward the analysis and design of complex integrated optical circuits of an arbitrary circuit diagram containing many paths and segments. Systems for analyzing and simulating electrical integrated circuits are many and well developed, as are computer-aided design systems for very large scale integration (VLSI) systems. An abstraction of design considerations has led to so-called *design rules,* such as the one stating that two parallel metal lines must be separated by a distance of at least 3λ, where λ corresponds to the smallest feature size of that technology (Ref. 21, p. 48).

The purpose of this study is to develop computer-aided analysis and design systems, together with similar abstractions as mentioned earlier. These, it is hoped, will make the realization of complex optical circuits possible.[22] In this paper, we will be concerned with analysis and simulation only, and will briefly mention how this analysis system can be made the basis of a design system. More concretely, we will report on a system that can calculate the loss and crosstalk for passive, single-mode, fairly complex channel waveguide circuits.

In the system developed, the signal and noise (undesired signal) levels of any point in the circuit are determined, given the topology of the circuit and the initial signal and noise levels at the inputs. The characteristic parameters of the waveguides, such as their propagation, attenuation, and coupling constants are also specified as inputs. The algorithm is very fast, so that adjustments can be made to improve the signal, noise, and crosstalk levels and the calculations repeated several times until a satisfactory signal-to-noise ratio (SNR) is achieved in all interconnects. Thus, it is a short step from our analysis/simulation system to the realization of a design system.

In Sec. 2, the problem is stated and the method of analysis is described. In Sec. 3, mathematical expressions for signal and noise calculations for different kinds of basic circuit features are given. The fast algorithms we developed are explained in Sec. 4. An example circuit with 15 paths is analyzed and the results are given in Sec. 5. The use of our method and possible further improvements are discussed in Sec. 6.

2 Problem Description and Approach

We analyze planar integrated optical circuits constructed of single-mode waveguides of arbitrary topology and complex-

Paper OIP-03 received May 28, 1993; revised manuscript received Dec. 15, 1993; accepted for publication Jan. 21, 1994.

ity, subject to the restrictions discussed later. Given the input signal and noise levels, we determine the output signal and noise levels. It is assumed that the circuits to be analyzed are rectilinear, so that the interconnects can be mapped on a Cartesian grid. We also assume that the interconnections are one-to-one; fan-out and fan-in are not allowed. Allowing such interconnections requires substantial modification of the developed procedures and algorithms, so that removal of this restriction is postponed for future research.

We assume that all of the waveguides are of the same width, geometry, and refractive index profile. The input is most likely a light source, and the output is most likely a light detector, both of which are probably situated on, or attached to, electronic integrated circuit chips. We do not make any assumptions regarding the nature of these transducers; any imperfect coupling into or out of the optical circuit is lumped into the efficiency factors η_{input} and η_{output}.

The light propagating in a waveguide is affected by bends, junctions, and neighboring guides. To calculate these effects as we go along a particular interconnection, we mentally divide the waveguide into what we call *segments,* which are elementary features of an interconnection. For coupling, only nearest neighbor waveguides are taken into consideration. This does not mean, however, that we totally disregard farther neighbor effects; the effect of a second-nearest neighbor is accounted for indirectly (since an undesired signal component coupled from the second-nearest to the nearest neighbor will have an effect on the total signal coupled into the waveguide under consideration, via the coupling from the nearest neighbor). Although this process is not exact, taking into account the coupling between each and every pair of circuit segments does not present itself as a formidable alternative, from both an analytical as well as a computational perspective. In any event, if a circuit is going to work properly, the overall coupling between paths must not exceed a small fraction of the signal level. This requirement means that for such a circuit, higher order coupling would usually be a much smaller fraction of the signal.

Segmentation is discussed further in Sec. 4.1. However, the simple circuit shown in Fig. 1 can help us understand the main idea. Each letter indicates a point where we break the interconnect into segments, thus we can refer to segments by letter pairs, such as CD. Some segments have a length, such as CD, JK. Others do not, such as BC, DE. The signal and noise levels associated with a segment are those at the ending point of it, thus the signal level of segment CD is the signal level at point D, s_D, and the noise level of the same segment is the noise level at the same point, n_D. The signal and noise levels correspond to the field amplitudes. As we propagate along a particular path, the signal level decreases due to attenuation and coupling losses. On the other hand, the noise level increases due to coupling from other paths. The signal and noise at a segment depend on those at the previous segment and those at the segments of the nearest neighboring waveguides. For example, the signal and noise levels at point B in Fig. 1 depend on the signal and noise levels at points A and L. Each path in the circuit is segmented individually, that is, segmentation is path dependent. During segmentation of a path, intersections and bends are noted, and the structure around the path is searched to find the nearest parallel waveguides on both sides. Any change in the structure of the neighboring guides indicates that the present segment has ended and a new segment should be created afterward. Hence, in a single segment, the neighboring waveguides, that is, the closest parallel guides, do not change their structure.

Segments are created with the purpose of isolating circuit features that are easily analyzed. As illustrated by our example, any circuit satisfying the previously mentioned assumptions can be broken down into five circuit features, that is, basic elements of the circuit, namely,

1. stretch of waveguide with no neighbors
2. stretch of waveguide with a neighbor on one side
3. stretch of waveguide with neighbors on both sides
4. orthogonal bend of a waveguide
5. orthogonal intersection of two waveguides.

For each interconnect, we start with a given signal and noise level at the input. Since the effect of each of the preceding circuit features is known, we can calculate the loss in signal power and the accumulation of undesired crosstalk by the time we reach the output. We work with two field amplitudes, one denoting signal level and one denoting noise. (Noise is defined so as to include all undesired coupling into the guide. If a detector is tied to the output, the thermal and shot noises associated with it must be added to the figure our system produces.)

Since we cannot expect that there will be a predetermined or fixed phase relationship between the various light sources, we assume that the phase relationships between the interacting signals are such so as to result in the greatest increase in noise and the greatest decrease in signal level. This type of worst-case analysis is necessary because the phases of the light sources may drift over time.

If the noise and signal levels of all neighboring interconnects were known to start with, one could calculate the signal and noise level at the output of a particular interconnect by working one's way along each segment, from the light source to the detector (i.e., from point A to point K in Fig. 1). However, to begin with, we do not have the signal and noise levels at any interconnect. Thus, a system of equations relating all of the signal and noise levels must be created and solved to obtain the desired output signal and noise levels:

$$\mathbf{x} = \mathbf{T}\mathbf{x} + \mathbf{I} \ , \tag{1}$$

where $\mathbf{x}$ is the vector whose elements are the signal and noise levels for all the segments, $\mathbf{T}$ is the matrix relating the signal and noise at any segment to those at previous segments and

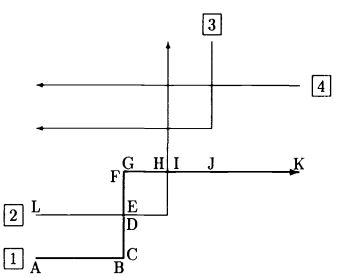

Fig. 1 Example circuit illustrating the process of segmentation. (Path numbers are labeled at the inputs. Arrows indicate the outputs.)

neighbors as explained in the next section, and **I** is the vector of input sources.

3 Signal and Noise Level Calculations for the Five Basic Circuit Features

For each interconnection path, starting from the source up to the detector, each segment can be modeled as one of the five elementary features mentioned in the previous section. The signal and noise calculations for these five circuit features are described next.

3.1 *Stretch of a Single Waveguide*

The attenuation is assumed to be uniform along a waveguide. Both signal and noise components are attenuated by a factor of $e^{-\alpha l}$, where α is the attenuation coefficient and l is the length of this segment of the guide. The following can be given as an example of the attenuation coefficient for Ti:$LiNbO_3$. The loss is 1 dB/cm at $\lambda = 0.633$ μm, 0.5 dB/cm at $\lambda = 1.15$ μm, and 0.2 dB/cm at $\lambda = 1.52$μm (Ref. 23, p. 224)

3.2 *Stretch of Two Parallel Waveguides*

Now we consider that on one side of the waveguide in consideration there is a parallel running waveguide.

In such a structure, if s_1 and n_1 are the signal and noise levels of the first guide at the input side of the segment, s_2 and n_2 are those of the second guide, l is the length of the parallel run along this segment, α is the attenuation coefficient along a waveguide, and κ is the coupling coefficient between the waveguides, then the signal and noise levels of the first guide at the output are given by the following equations (Ref. 24, p. 626):

$$s_1' = s_1|\cos(\kappa l)|e^{-\alpha l} , \tag{2}$$

$$n_1' = [n_1|\cos(\kappa l)| + (s_2 + n_2)|\sin(\kappa l)|]e^{-\alpha l} . \tag{3}$$

The $e^{-\alpha l}$ term is related to attenuation. The cosine term accounts for the fact that part of the signal is out-coupled to the other guide. The sine term accounts for the fact that the signal and noise propagating in the other guide is coupled into the first guide. This undesired coupling accumulates as noise. As mentioned before, we are assuming the worst possible phase relation between the light propagating in both guides.

We must mention an approximation inherent in this method of analysis. As illustrated in Fig. 2, light propagating inside guide 1 interacts with light propagating in both the horizontal and the vertical portions of guide 2. The effect of interaction with the vertical portion is somewhat analogous to the fringing effect in a parallel plate capacitor. As long as the distance of parallel interaction is long, the fringe effect can be neglected with small error. (If the distance of parallel interaction is small, this would mean that the overall coupling over this segment of the interconnect is small compared to other segments, so that again the error is small.)

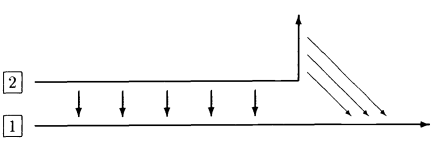

Fig. 2 The fringing effect from the second guide to the first one is neglected.

3.3 *Stretch of Three Parallel Waveguides*

Generally, a straight running waveguide, unobstructed by bends or intersections, will have neighboring waveguides on both sides. Most segments will be of this type.

In a structure of three parallel waveguides, if s_1, s_3 and n_1, n_3 are the signal and noise levels of the outer guides at the input, respectively, s_2 and n_2 are those of the center guide, l is the length of the waveguides, and α is the attenuation coefficient along a waveguide, the signal and noise levels of the center guide at the output are given by the following expressions (Refs. 25, pp. 136–137, and 26):

$$s_2' = s_2|\cos(\kappa l)|e^{-\alpha l} , \tag{4}$$

$$n_2' = \left[n_2|\cos(\kappa l)| + (s_1 + n_1)\frac{\kappa_{12}}{\kappa}|\sin(\kappa l)| + (s_3 + n_3)\frac{\kappa_{23}}{\kappa}|\sin(\kappa l)| \right] e^{-\alpha l} , \tag{5}$$

where $\kappa = (\kappa_{12}^2 + \kappa_{23}^2)^{1/2}$, κ_{ij} is the coupling coefficient between waveguide i and waveguide j, where $(i,j) = \{(1,2),(2,3)\}$.

3.4 *Orthogonal Bend*

In most cases, each interconnection will suffer from at least one 90-deg bend. Smooth curved bends take up too much space, requiring as much as a 1-cm radius in weakly guiding waveguides in Ti:$LiNbO_3$. Obviously, this limits the packing density considerably. For this reason, for right or left turns, total internal reflection mirrors, as in Fig. 3, are assumed. Due to the large index difference between core and air at the corner, the reflection coefficient is very close to unity (Ref. 23, p. 229). Such a bend can be characterized by an efficiency factor η_b, which accounts for the power loss as a result of the bend. Therefore, if the signal and noise levels before an orthogonal bend are s_1 and n_1, respectively, then those after the bend, s_1' and n_1', respectively, are given by

$$s_1' = \sqrt{\eta_b}\, s_1 , \tag{6}$$

$$n_1' = \sqrt{\eta_b}\, n_1 . \tag{7}$$

3.5 *Orthogonal Intersection*

Unless multilayer optical circuits can be realized, intersection of waveguides will be unavoidable. The loss and crosstalk is very angle sensitive and the loss is minimal for normal

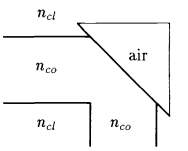

Fig. 3 Orthogonal bend implemented by total internal reflection.

intersection, which is the only kind possible for rectilinear circuits anyway. This feature can be characterized by two parameters, one accounting for the insertion loss (η_i) and the other for crosstalk (η_c). Thus, the signal and noise levels in the horizontal waveguide in Fig. 4 can be calculated by using the following equations:

$$s_1' = \sqrt{\eta_i} s_1 \ , \tag{8}$$

$$n_1' = \sqrt{\eta_i} n_1 + \sqrt{\eta_c}(s_2 + n_2) \ . \tag{9}$$

4 Computer Analysis and Simulation

In this section, we describe the algorithm and computer implementation of the analysis described earlier. Although the process of segmentation and calculation of crosstalk and coupling is easy to grasp intuitively, development of the appropriate data structures and procedures that result in a fast analysis system is not straightforward. Only a brief description of the algorithm and implementation is given here; details are documented in Ref. 27.

The circuit topology is represented in the form of three different data structures. The information stored in these data structures is partially redundant, however, each is structured in a particular way so as to be efficiently accessed by the various search procedures in the algorithm. They are all *arrays-of-pointers* type data structures and store the circuit topology in the following manner:

1. In the first one, each pointer in the array represents a path and each cell of the pointer corresponds to an orthogonal bend along this path. For example, for the circuit shown in Fig. 1 the first pointer of the array contains the information about the first path in the circuit (see Fig. 5). The first cell of the pointer maintains the coordinates of point A (A_x is the abscissa of point A and A_y is the ordinate of the same point in Fig. 5), which is the input of the path. In the same manner, the second cell is for the coordinates of point B, the third cell is for those of point F, and the last cell is for point K, which is the output. A total of four cells exists in the pointer and they are in the correct order from the input to the output.

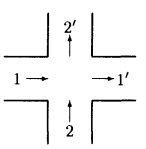

Fig. 4 An orthogonal intersection. Arrows represent direction of light.

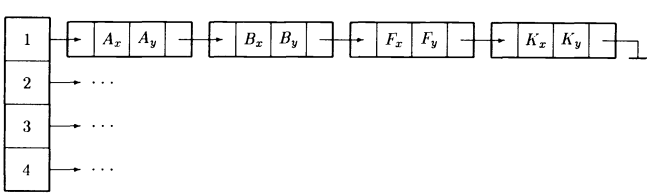

Fig. 5 First array-of-pointers type data structure for the circuit in Fig. 1.

2. Each element of the second array corresponds to a horizontal line, that is, a row, in the Cartesian grid in which the circuit is embedded. Each cell of a pointer is a horizontal line segment between two consecutive corners of a path lying on the corresponding row. The cells of the pointers are sequenced with respect to the abscissa of the left starting point of the horizontal line segment. The first pointer of the array represents the lowest horizontal line of the rectilinear Cartesian plane containing the circuit. In the circuit shown in Fig. 6, let us assume that the inputs of the first and third paths are located on row 1. Then the first pointer of the array represents all the horizontal line segments lying on this row (see Fig. 7). The first cell contains the information about the first line segment AB on this row, namely the abscissa of points A and B (A_x and B_x, respectively) and the path number to which these segments belong (which is 1). The second cell contains the abscissa of points C and D (C_x and D_x, respectively) and the path number (which is 2). The third cell contains the abscissa of points E and F and the path number (which is 3). There are in total three cells in the pointer and they are in the correct order from left to right. There is no interconnect in the second row of the circuit shown in Fig. 6, therefore, the pointer corresponding to the second element of the array is simply a nil pointer (see Fig. 7). In the circuit, there is only one horizontal interconnect in the third row, thus, the pointer belonging to the third element of the array has only one cell. The rest of the array is created in the same manner.
3. The third array is very similar to the second array but stores the vertical line segments instead of horizontal ones.

4.1 *Segmentation Algorithm*

The segmentation of each interconnect path is the most important part of the program. A segment is defined as a part of an interconnect path that forms one of the basic circuit

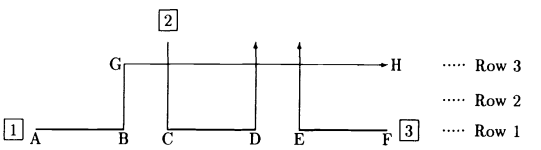

Fig. 6 Example circuit illustrating the creation of array-of-pointers type data structures. (Path numbers are labeled at the inputs. Arrows indicate the outputs.)

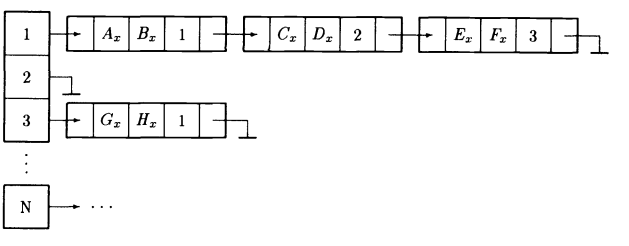

Fig. 7 Second array-of-pointers type data structure for the circuit in Fig. 6; *N* is the total number of rows in the rectilinear plane in which the circuit is embedded.

features described in Sec. 3 (see also Fig. 1). The signal and noise levels at any segment of a path depend on those at the previous segment of the same path and those at neighboring interconnects.

The segmentation algorithm starts from the source at the first path and continues toward the detector of this path. When segmentation of the first path is finished, the algorithm continues with the second path, third path, etc. At the end of the algorithm, the path number, orientation, signal flow direction, coordinates, distances to neighbors, and signal flow directions of the neighbors for each segment are stored.

The algorithm starts by storing the source and corner points of each path, which are conveniently available in the first array of pointers, shown in Fig. 5. This process corresponds to the first step in segmentation. The portion of a path running between two corners must be further segmented depending on neighboring parallel paths. (For instance, the portion AE in Fig. 8 will be further segmented into AB, BC, CD, and DE.) This is accomplished by using the following algorithm.

Again we refer to Fig. 8 as an example. In the second array of pointers, shown in Fig. 7, the rows just above and just below the one containing the portion (AE) of the path to be segmented, that is, the previous element in the array, is searched for a line segment whose x coordinates may overlap with those of the path to be segmented. If such a line segment exists, the x coordinates describing the extent of overlap and the distance between the two lines are stored in a single cell of a newly created pointer-type data structure. In the figure, an overlap extending over the portion AB is detected. In this case, parallel runs exist both above and below the segment AB, so that this part of the path is treated as a stretch of waveguide with neighbors on both sides. We now continue working on the remaining portion BE.

The algorithm continues searching for possible overlaps in the neighboring rows of the array of pointers of Fig. 7 and comes across the parallel run just above BC. This time, on the lower side, we do not come across a parallel run within a preset distance, so that the segment BC is designated as a stretch of waveguide with a neighbor on one side only. Then, the algorithm continues searching farther and farther rows in the data structure of Fig. 7, until it comes across the parallel run above CD, which is also treated as a single neighbor run. Finally, DE is recognized as a segment due to the parallel run on both sides. Thus, AE has been broken down into the four segments AB, BC, CD, and DE. In some cases, unlike in this example, the segments may not be recognized in the correct order (for instance, DE may be recognized before CD). Nevertheless, they are stored in the proper order by the algorithm. Then, the information corresponding to these segments, in the correct order, is inserted in between the information corresponding to the corners A and E, which were already recognized as segments. Then, the algorithm continues with segmentation of line portions between other bends and intersections of the path. In the end, the information pertaining to the segments is stored in the correct order, as we come across them along the path.

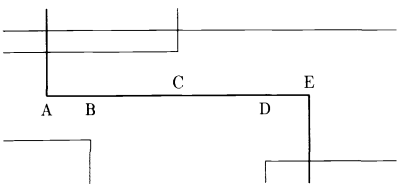

Fig. 8 Segmentation algorithm for a line segment AE after the neighbors are determined in both directions.

4.2 *Self-consistent Solution of the Signal and Noise Levels*

After all the interconnect paths are segmented, the **x** and **I** vectors and the **T** matrix of Eq. (1) can be created. The elements of the vector **x** are the signal and noise values associated with the segments. This vector is the unknown vector to be solved in Eq. (1). Vector **I** contains the signal and noise values of the input sources. Matrix **T** contains the coefficients relating the signal or noise values of a segment to those of the previous segments on the same path, and of segments of neighboring paths.

All the information necessary to calculate the coefficients of the matrix **T** can be obtained from the results of the segmentation algorithm (see Sec. 4.1), which contains the coordinates, separations, etc. of the segments, all properly labeled and ordered. For instance, if a segment involves parallel waveguides in both directions, we use the formula given in Sec. 3 to obtain the related coefficient of the matrix **T**, in terms of the length and separation of the parallel run.

Then, the signal and noise values for every segment in the circuit are computed by

$$\mathbf{x} = (\mathbf{I} - \mathbf{T})^{-1}\mathbf{I} \ , \tag{10}$$

where **I** is the identity matrix. At most, two neighboring paths are coupled to the segment under consideration, therefore, the matrix $\mathbf{I} - \mathbf{T}$ has at most six nonzero elements in any row. Thus, very fast solution of Eq. (10) is possible by using sparse matrix algorithms.

It should be emphasized that the method of analysis and simulation discussed until now is independent of how the attenuation, propagation, and coupling parameters of the waveguides are calculated. These should be considered simply as inputs to our system. The exact profile or refractive index distribution are not relevant for our programs; their effect is summarized in the mentioned parameters. Such parameters may be numerically calculated[28] or even experimentally determined. An analytic approach for calculation of these parameters for step index channel waveguides and the extension to waveguides of arbitrary profile are given in Refs. 27, 29, and 30.

4.3 *Computer Implementation*

The described algorithm has been implemented on a personal computer with the PASCAL programming language, with the exception of the sparse matrix solver, which was written in the C language. In this implementation, the user enters the circuit to be analyzed by means of a cursor-driven interface. The spacing of the Cartesian grid is specified by the user. While the circuit topology is being entered, the three different data structures described in Sec. 4 are created simultaneously. The user also inputs the attenuation coefficient, coupling coefficient, and the similar parameters for bends and intersections, and also the wavelength of light. Once these parameters are entered, the signal and noise levels at any point

in the circuit can be determined in terms of the signal and noise levels at the sources. The program run is of the order of a few seconds for the circuit in Fig. 9.

An auxiliary program has also been developed that can calculate the coupling and other parameters in terms of the physical parameters of the waveguides, such as its dimensions, refractive indices, etc., for channel waveguides. In the program, the efficiency factor η_b and insertion loss η_i discussed in Secs. 3.4 and 3.5, respectively, are approximated by the percentage of power propagating in the core (η) as calculated in Ref. 28, p. 243. For arbitrary waveguide profiles, the values of η_b and η_i can be replaced by η of Ref. 28, p. 257. Thus, the user has a choice of entering the circuit parameters or the physical waveguide parameters.

5 Examples and Results

For the purpose of illustration we present results for the circuit shown in Fig. 9 with 15 paths. This particular circuit turned out to have 320 segments.

The channel waveguide interconnects in the circuit (see Fig. 10) have a width w of 1 μm, a thickness t of 0.7 μm, a signal attenuation constant of 100 m^{-1}, and refractive indices of 3.5 in the core ($n_1 = 3.5$), 3.35 in the cladding region ($n_2 = n_3 = 3.35$), and 3.43 in the lateral direction ($n_4 = n_5 = 3.43$). The wavelength of light is assumed to be 1.5 μm. The spacing of the grid lines on which the circuit is laid out has been taken as twice the width of a waveguide (2 μm).

As the first example, the minimum spacing between the nearest waveguides is taken as three times the grid spacing (6 μm). The coupling coefficient is calculated (Ref. 31, p. 52) and found to be $\kappa = 7.022 \times 10^{-2}\ m^{-1}$. The orthogonal bend and intersection parameters are found to be $\eta_b = \eta_i = 0.4614$ (see Sec. 4.3). The intersection crosstalk parameter η_c is assumed to be small enough that it can be taken as zero.

We assume the signal and noise levels at the inputs to be 1 and 10^{-4}, respectively (in arbitrary units). The corresponding signal and noise levels and SNRs at the outputs are given in Table 1.

The lowest output SNR occurred for path 12 and is equal to 40.99. Note that this is one of the longest paths and has the most number of bends. Remember that the noise level given in Table 1 does not include the thermal and shot noises associated with the detector and related circuitry. These can be easily accounted for, depending on the type of detector and circuitry used.

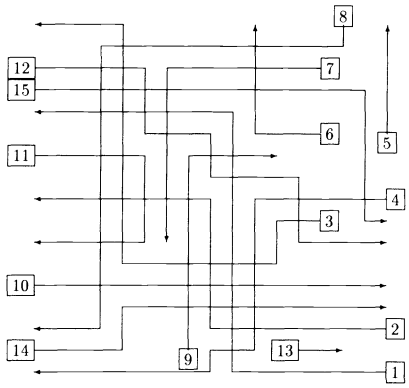

Fig. 9 Example circuit with 15 paths and 320 segments.

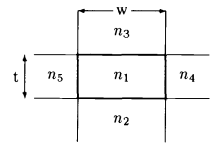

Fig. 10 General step index channel waveguide.

Table 1 Output signal, noise, and SNR values of the example circuit.

Output number	Signal level	Noise level	Output SNR
1	0.0005369	2.050×10^{-7}	2619
2	0.0009601	7.878×10^{-7}	1219
3	0.00009487	1.942×10^{-6}	48.85
4	0.001710	2.512×10^{-6}	680.7
5	0.9975	9.975×10^{-5}	10^4
6	0.09862	1.020×10^{-5}	9669
7	0.03092	5.950×10^{-6}	5197
8	0.0009572	5.144×10^{-7}	1861
9	0.01736	1.188×10^{-5}	1461
10	0.05510	3.078×10^{-5}	1790
11	0.01735	3.413×10^{-6}	5084
12	0.0001693	4.130×10^{-6}	40.99
13	0.9990	9.990×10^{-5}	10^4
14	0.03088	2.834×10^{-5}	1090
15	0.009696	4.682×10^{-6}	2071

The circuit design can be modified if some of the output SNRs are not large enough. A simple way of achieving this is to increase the separation between the waveguides. For instance, let us increase the minimum spacing between the nearest waveguides to five grid spacings (10 μm) in the previous circuit. In this case, the coupling coefficient becomes $\kappa = 7.354 \times 10^{-6}\ m^{-1}$. The output signal and noise levels for this case are given in Table 2. The path with the minimum output SNR is again path 12, but the SNR is now 9561. This significant increase in the output SNR is a result of the exponential dependence of coupling on the separation of the guides.

A more intelligent (but much more involved) design procedure would be to selectively increase the separation between those guides that do not exhibit satisfactory SNR rather than increasing all separations uniformly as we have done earlier. Thus, it is possible to achieve a minimum circuit area for a specified SNR.

6 Conclusions, Discussion, and Future Work

We have developed a method of analysis for integrated optical circuits of arbitrary topology. A system based on this method has been implemented. It calculates signal and noise

Table 2 Output signal, noise, and SNR values of the example circuit with increased grid spacing.

Output number	Signal level	Noise level	Output SNR
1	0.0005309	5.312×10^{-8}	9994
2	0.0009516	9.529×10^{-8}	9986
3	0.00009389	9.759×10^{-9}	9621
4	0.001693	1.698×10^{-7}	9971
5	0.9955	9.955×10^{-5}	10^4
6	0.09830	9.830×10^{-6}	10^4
7	0.03074	3.074×10^{-6}	10^4
8	0.0009465	9.473×10^{-8}	9992
9	0.01727	1.729×10^{-6}	9988
10	0.05474	5.479×10^{-6}	9993
11	0.01726	1.726×10^{-6}	10^4
12	0.0001677	1.754×10^{-8}	9561
13	0.9982	9.982×10^{-5}	10^4
14	0.03066	3.070×10^{-6}	9987
15	0.009611	9.618×10^{-7}	9993

levels at the output of each interconnect, given those at the input. Novel data structures and algorithms for storing and manipulating the circuit have been created in the process.

Because of its speed, our analysis system can be made the basis of a design system in a straightforward manner. One can start with a relatively densely packed circuit. After running our analysis program, the spacing between interconnects that result in unsatisfactory SNRs and their neighbors can be increased. This process can be iterated until a satisfactory SNR is achieved for all interconnects. An alternative approach would be to start from a well-spaced circuit, and then try to compact it using our analysis system.

Empirical studies of a large number of circuits can lead to several general design rules, as well as general guidelines, experience, and intuition as to how such circuits should be contemplated and laid out in the first place. This would be of great value, since design tools for systems of such complexity usually converge to local optima, and how close we are to the globally optimum circuit layout depends on the initial layout with which we start the optimization.

A useful measure of the packing density of any given circuit is the ratio of the total area A to the total length of interconnections l_{total}, which can be interpreted as the effective transverse width of interconnections, which also accounts for all inefficiencies in packing the lines. Normalizing by the wavelength of light used,

$$w_{\text{eff}} = \frac{A}{l_{\text{total}} \lambda} \quad . \tag{11}$$

The value of w_{eff} for the circuit given in Fig. 9 is 3.86 for a minimum separation of 6 μm, and 6.44 for a minimum separation of 10 μm. (No effort has been made to compact this circuit as much as possible.) Naturally, w_{eff} cannot be made smaller than unity. In general, there will be a trade-off between w_{eff} and the SNR.

Apart from the developments suggested earlier, future work may include experimental verification of the results of the program for a trial circuit similar to that given in Fig. 9 and extension to circuits with fan-out and fan-in.

Acknowledgments

We are grateful to Ogan Ocali of Bilkent University for letting us benefit from his expertise in solving sparse matrix equations and providing us with the necessary programs. We extend our thanks to Tülay Çora, Tuncer Demirel, and Baki Şahin, who did a major part of the programming. Their efficient programming contributed to the speed of operation of our system. This research was sponsored by NATO's Scientific Affairs Division in the framework of the Science for Stability Programme.

References

1. J. W. Goodman, F. J. Leonberger, S. Y. Kung, and R. A. Athale, "Optical interconnections for VLSI systems," *Proc. IEEE* **72,** 850–866 (1984).
2. L. D. Hutcheson and P. Haugen, "Optical interconnects replace hardware," *IEEE Spectrum,* pp. 30–35 (March 1987).
3. R. K. Kostuk, J. W. Goodman, and L. Hesselink, "Optical imaging applied to microelectronic chip-to-chip interconnections," *Appl. Opt.* **24,** 2851–2858 (1985).
4. J. A. Neff, "Major initiatives for optical computing," *Opt. Eng.* **26**(10), 2–9 (1987).
5. H. M. Ozaktas, "A physical approach to communication limits in computation," PhD Thesis, Stanford University (June 1991).
6. H. M Ozaktas and J. W. Goodman, "Implications of interconnection theory for optical digital computing," *Appl. Opt.* **31,** 5559–5567 (1992).
7. H. M. Ozaktas and J. W. Goodman, "The limitations of interconnections in providing communication between an array of pointers," in *Frontiers of Computing Systems Research,* pp. 61–130, Plenum Press, New York (1991).
8. M. R. Feldman, S. C. Esener, C. C. Guest, and S. H. Lee, "Comparison between optical and electrical interconnects based on power and speed considerations," *Appl. Opt.* **27,** 1742–1751 (1988).
9. F. E. Kiamilev, P. Marchand, A. V. Krishnamoorthy, S. C. Esener, and S. H. Lee, "Performance comparison between optoelectronic and VLSI multistage interconnection networks," *J. Lightwave Technol.* **9,** 1674–1692 (1991).
10. H. B. Bakoglu, *Circuits, Interconnections and Packaging for VLSI,* Addison-Wesley, Reading, MA (1990).
11. P. R. Haugen, S. Rychnovsky, A. Husain, and L. D. Hutcheson, "Optical interconnects for high speed computing," *Opt. Eng.* **25**(10), 1076–1085 (1986).
12. K. C. Saraswat and F. Mohammadi, "Effect of scaling of interconnections on the time delay of VLSI circuits," *IEEE Trans. Electron Devices* **29,** 645–650 (1982).
13. J. W. Parker, "Optical interconnection for advanced processor systems: a review of the ESPRIT 2 OLIVES program," *J. Lightwave Technol.* **9,** 1764–1773 (1991).
14. H. Kogelnik, "Theory of optical waveguides," in *Guided-Wave Optoelectronics,* Chap. 2, T. Tamir, Ed., Springer-Verlag, Berlin (1988).
15. W. Stutius and W. Streifer, "Silicon nitride films on silicon for optical waveguides," *Appl. Opt.* **6,** 3218–3222 (1977).
16. J. M. Trewhella et. al, "Polymeric optical waveguides," *Proc. SPIE* **1177,** 379–386 (1989).
17. B. L. Booth, "Lowloss channel waveguides in polymers," *J. Lightwave Technol.* **7,** 1445–1453 (1989).
18. C. S. Li, C. M. Olsen, and D. G. Messerschmitt, "Analysis of crosstalk penalty in dense optical chip interconnects using single-mode waveguides," *J. Lightwave Technol.* **9,** 1693–1701 (1991).
19. Y. Chung and N. Dagli, "An assessment of finite difference beam propagation method," *IEEE J. Quantum Electron.* **26,** 1335–1339 (1990).
20. R. Boult, "Simulation software aids optoelectronic research," *Lightwave,* PennWell Books, p. 14 (Mar. 1993).
21. C. Mead and L. Conway, *Introduction to VLSI Systems,* Addison-Wesley, Reading, MA (1980).
22. H. M. Ozaktas, "Research directions in integrated guided wave optical interconnects," Internal Report, Information Systems Laboratory, Stanford University, Palo Alto, CA (May 1989).

23. R. Sims and J. Cozens, *Optical Guided Waves and Devices,* McGraw-Hill, Shoppenhangers Road, Maidenhead, Bershire, England (1992).
24. A Yariv, *Quantum Electronics,* John Wiley & Sons, New York (1989).
25. W. K. Burns and A. F. Milton, "Waveguide transitions and junctions," in *Guided-Wave Optoelectronics,* Chap. 3, T. Tamir, Ed., Springer-Verlag, Berlin (1988).
26. K. Kishioka, "Improvement of the power spectral response in the three-guided coupler demultiplexer," *Appl. Opt.* **29,** 360–366 (1990).
27. Gurkan Onal, "Computer aided analysis and simulation of complex passive integrated optical circuits," Master's Thesis, Bilkent University, Ankara, Turkey (1993).
28. A. W. Snyder and J. D. Love, *Optical Waveguide Theory,* Chapman and Hall, New York (1983).
29. G. Onal, A. Altintas, and H. Ozaktas, "A study of development of design rules for photonic chips," in *Lightwave Technology and Communications,* A. Altintas and G. Saplakoglu, Eds., pp. 235–241, Bilkent University, Ankara, Turkey (July 1992).
30. R. J. Black and C. Pask, "Equivalent optical waveguides," *J. Lightwave Technol.* **2,** 268–276 (1984).
31. T. K. Findakly, "Optical channel waveguides and waveguide couplers," in *Handbook of Microwave and Optical Components,* Chap. 2, K. Chang, Ed., John Wiley & Sons, New York (1989).

Gürkan Önal received his BS and MS degrees from the Department of Electrical and Electronics Engineering, Bilkent University, Ankara, in 1991 and 1993, respectively. He is currently studying for his PhD degree and is working as a research assistant in the same university. His interests include optical systems and integrated optics.

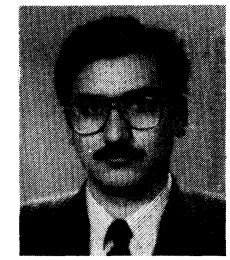

Ayhan Altintaş received his BS and MS degrees from the Middle East Technical University (METU), Ankara, Turkey, in 1979 and 1981, respectively, and the PhD degree from Ohio State University, Columbus, in 1986, all in electrical engineering. From 1981 to 1987, he was with the ElectroScience Laboratory, Ohio State University. He then spent one year at the Optical Sciences Center of The Australian National University, Canberra. Currently, he is an associate professor at the Department of Electrical and Electronics Engineering, Bilkent University, Ankara, Turkey. His research interests are in electromagnetic radiation and scattering, microwaves, fiber optics, and integrated optics. Dr. Altintaş is a senior member of IEEE and a member of Sigma Xi and Phi Kappa Phi. He is the recipient of the ElectroScience Laboratory Outstanding Dissertation Award of 1986, the IEEE 1991 Outstanding Student Branch Counselor Award, and the 1991 Research Award of the Professor Mustafa N. Parlar Foundation of METU.

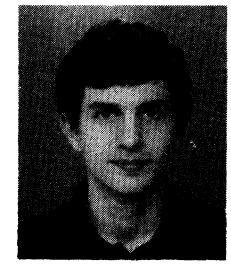

Haldun M. Ozaktas received a BS degree from the Middle East Technical University, Ankara, Turkey, in 1987 and MS and PhD degrees from Stanford University, California, in 1988 and 1991, respectively, all in electrical engineering. His academic interests include optical information processing, optical interconnections, and signal processing. He is currently an assistant professor of electrical engineering at Bilkent University, Ankara, Turkey.